Hollow carbon spheres in microwaves: Bio inspired absorbing coating

D. Bychanok, S. Li, A. Sanchez-Sanchez, G. Gorokhov, P. Kuzhir, F. Y. Ogrin, A. Pasc, T. Ballweg, K. Mandel, A. Szczurek, V. Fierro, and A. Celzard

Citation: Applied Physics Letters **108**, 013701 (2016); doi: 10.1063/1.4938537

View online: http://dx.doi.org/10.1063/1.4938537

View Table of Contents: http://scitation.aip.org/content/aip/journal/apl/108/1?ver=pdfcov

Published by the AIP Publishing

Hollow carbon spheres in microwaves: Bio inspired absorbing coating

D. Bychanok,[1,a)] S. Li,[2] A. Sanchez-Sanchez,[3] G. Gorokhov,[1] P. Kuzhir,[1] F. Y. Ogrin,[4] A. Pasc,[2] T. Ballweg,[5] K. Mandel,[5,6] A. Szczurek,[3] V. Fierro,[3] and A. Celzard[3]
[1]*Research Institute for Nuclear Problems BSU, 11 Bobruiskaya Str., 220030 Minsk, Belarus*
[2]*NANO Group, SRSMC-UMR Université de Lorraine-CNRS 7565, Vandoeuvre-lès-Nancy Cedex, France*
[3]*Institut Jean Lamour-UMR Université de Lorraine-CNRS 7198, ENSTIB, 27 rue Philippe Seguin, CS 60036, 88026 Epinal Cedex, France*
[4]*University of Exeter, Exeter EX4 4QL, United Kingdom*
[5]*Fraunhofer Institute for Silicate Research ISC, Neunerplatz 2, 97082 Wuerzburg, Germany*
[6]*Julius-Maximilians-University Wuerzburg, Chair of Chemical Technology of Materials Synthesis, Roentgenring 11, 97070 Wuerzburg, Germany*

(Received 18 November 2015; accepted 11 December 2015; published online 5 January 2016)

The electromagnetic response of a heterostructure based on a monolayer of hollow glassy carbon spheres packed in 2D was experimentally surveyed with respect to its response to microwaves, namely, the Ka-band (26–37 GHz) frequency range. Such an ordered monolayer of spheres mimics the well-known "moth-eye"-like coating structures, which are widely used for designing anti-reflective surfaces, and was modelled with the long-wave approximation. Based on the experimental and modelling results, we demonstrate that carbon hollow spheres may be used for building an extremely lightweight, almost perfectly absorbing, coating for Ka-band applications. © *2016 AIP Publishing LLC*. [http://dx.doi.org/10.1063/1.4938537]

Porous structures based on glasslike carbon, whether in the form of foams, periodic architectures, or gels, have attracted the attention of many researchers due to their outstanding combination of physical properties.[1–7] Unlike most random carbon foams, for which it is still challenging to accurately control geometric parameters, hollow carbon spheres can be more easily tailored through a synthesis method based on well-calibrated sacrificial templates. This advantage turns such spheres into very interesting candidates for using them in electromagnetic applications.

In particular, hollow spheres (HS) made of glasslike carbon with uniform diameter can be potentially used for producing ordered periodic structures. In this work, the electromagnetic properties of a system formed by a single layer of carbon HS packed in 2D were investigated. Its structure is similar to a well-known type of anti-reflective surfaces having a "moth-eye"-like structures.[8–10] In the present case, however, the HS monolayer is an electrically conductive material with losses; thus, due to these attractive properties, it may be used for EM absorption applications. With this aim in view, the long-wave approximation, used for modelling structures presenting a spatial dispersion of refractive index,[9] was adapted to the description of the HS monolayer response in microwaves. For calculating reflection R, transmission T, and absorption A coefficients of the HS monolayer, the model of wave distribution in multi-layered medium, widely used in optics,[11] was applied.

Carbon HS samples were prepared by a template method based on two kinds of sacrificial spherical polymer beads, having two different diameters. As both present a nearly zero carbon yield when directly pyrolysed at 900 °C under inert atmosphere, hydrothermal conditions were used for depositing a sucrose-derived hydrochar at their surface. The resultant spheres were next converted into glasslike carbon through an additional subsequently pyrolysis step at 900 °C in nitrogen flow. During such heating, the initial material of the spheres was largely destroyed so that both kinds of HS can be considered as purely made from the same carbon derived from sucrose. In the following, the carbon hollow spheres are referred to as HS-A and HS-B, the former having a lower diameter than the latter (see Table I).

Scanning electron microscopy images of the two kinds of HS discussed here are presented in Fig. 1. Pictures showing damaged spheres were deliberately chosen to demonstrate their hollow character, but the vast majority of carbon HS was neither broken nor cracked.

The dimensions of several tens of carbon HS were measured by electron microscopy, using full particles for average diameter determination. For further calculations, we assume that carbon spheres consist of glassy carbon with a density $\rho = 1.55\ \mathrm{g/cm^3}$ and a static conductivity $\sigma = 20\,000\ \mathrm{S/m}$.[12–14] For microwave characterisation, the spheres were assembled in monolayers. The average shell thickness of the spheres was deduced from the known values of density of glassy carbon, weight and number of spheres in the monolayer, and average sphere diameter. All these physical parameters of spheres and monolayers are collected in Table I.

The electromagnetic response of a monolayer based on each kind of carbon hollow spheres was investigated in the Ka-band (26–37 GHz). All measurements were performed in a 7.2×3.4 mm waveguide system. In a typical experiment, the spheres were initially packed to form a close-compact layer which was then placed inside the waveguide between two 1 mm-thick layers of transparent to microwave Styrofoam®.

Due to the unavoidable, slight distribution of HS sizes and due to some defects in the packing of such lightweight, fragile objects, the as-obtained 2D ordering was closer to a square-shaped lattice.

The microwave measurements were carried out using the scalar network analyser ELMIKA R2-408R. The EM

a)dzmitrybychanok@ya.ru

TABLE I. Parameters of carbon hollow spheres (HS) and monolayers (ML) based on them.

Name	Diameter, mm	Wall thickness, μm (calculated)	ML weight,mg	Number of spheres in ML
HS-A	1.34	14.3	2.2	18
HS-B	1.85	27.8	2.7	6

responses of the samples were obtained as ratios of transmitted to input (S_{21}) and reflected to input (S_{11}) signals.

The simplified geometry, assumed for investigating the monolayers based on two separate sizes of carbon hollow spheres, is the one presented in Fig. 2. The wavelength of the radiation in the Ka-band, 1 cm at 30 GHz, is much larger than the HS diameter. This allowed to apply long-wave approximation widely used in optics for modelling anti-reflective coatings.[8–10] This approximation allows introducing a homogenisation procedure to calculate the spatial dispersion of the effective refractive index of the monolayer formed by the 2D packed lattice of spheres (see below). Therefore, the investigated system can be considered as a stack of thin layers of constant refractive index so that the characteristic matrix of the corresponding assembly of thin films can be calculated and directly converted into reflection $R = S_{11}^2$ and transmission $T = S_{21}^2$ coefficients. The equations below were written using SI units and assume an $\exp[i\omega t - ikz]$ harmonic time convention.

Let us consider the cross-section of a HS monolayer along the yz-plane at the coordinate $x = x_0$, where $|x_0| < r_o$, where r_o is the outer sphere radius, as shown in Fig. 2(b). This cross-section consists of ring-like carbon regions and air regions. The homogenisation procedure in this case means that the non-conductive air regions can be averaged with highly conductive carbon regions according to their relative surface fractions. The symmetry of the system allows considering just one unit cell which is a square of side $\tau = 2r_o$. For calculating the surface fractions of carbon and air regions parallel to the yz-plane at the coordinate x_0, let us consider a cross-section of a hollow sphere along the xz-plane, as presented in Fig. 2(b). From this figure, it can be easily calculated that the glassy carbon ring surface area is $S(x_0) = \pi(r_o^2 - x_0^2) - \pi(r_i^2 - x_0^2)$, whereas that of air is $4r_o^2 - S(x_0)$ along the yz-plane at the coordinate x_0. The dependence of $S(x_0)$ on x_0 vanishes when $|x_0| < r_i$, where r_i is the inner radius of HS (in the center region terms with x_0 cancel out and $S(x_0) = S(r_i)$). Averaging inside the unit cell directly leads to the following equation for the refractive index:

$$n(\nu, x) = [n_s(\nu)S(x) + n_0(4r_o^2 - S(x))]/(4r_o^2), \quad (1)$$

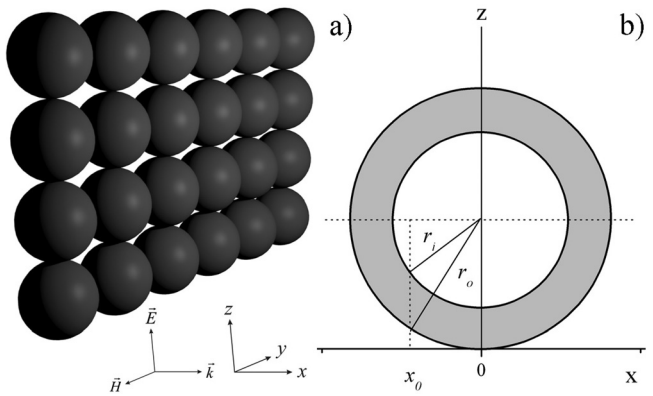

FIG. 2. (a) Geometry of a carbon hollow spheres monolayer, and (b) cross-section of a single sphere of outer and inner radii r_o and r_i, respectively, along the xz-plane.

where

$$S(x) = \begin{cases} \pi(r_o^2 - r_i^2), & |x| \le r_i \\ \pi(r_o^2 - x^2), & r_o \ge |x| > r_i \\ 0, & |x| > r_o, \end{cases} \quad (2)$$

and where $n_s(\nu) = \sqrt{1 - \frac{i\sigma}{2\pi\nu\varepsilon_0}}$ is the refractive index of carbon, i being the imaginary unit, $\sigma = 20\,000$ S/m the static conductivity of glassy carbon, ν the frequency, $\varepsilon_0 = 8.85 \times 10^{-12}$ F/m is the permittivity of vacuum, and $n_0 = 1$ the refractive index of air.

Thus, the EM response of a monolayer of carbon HS in the long-wave approximation is considered as equivalent to that of a layer of bulk material of thickness $\tau = 2r_o$ and with a spatial dispersion of refractive index which obeys Equation (1).

Fig. 3 shows such spatial dispersions (1) for bulk and hollow spheres. The void inside the spheres leads to a constant refractive index in the central region of the HS monolayer.

The maximum values of the refractive index of bulk (index b) and hollow (index h) spheres are, respectively

$$n_b(\nu) = \pi n_s(\nu)/4 - n_0(1 - \pi/4), \quad (3)$$

$$n_h(\nu) = [n_s(\nu)\pi(r_o^2 - r_i^2) + n_0(4r_o^2 - \pi(r_o^2 - r_i^2))]/(4r_o^2). \quad (4)$$

It is worth noticing that, within the long wave approximation, the type of ordering of HS in the monolayer does not significantly affect the EM absorption properties, unlike, for example, changes of HS shell thickness.

For calculating the EM response of the HS monolayer, the model of wave distribution in a multi-layered medium[11] was used. Let us consider a layer of bulk material with the

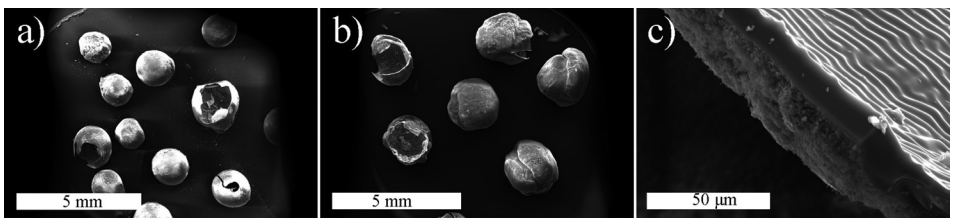

FIG. 1. SEM images of carbon hollow spheres: (a) A-series and (b) B-series, shell edge (c) of a broken sphere.

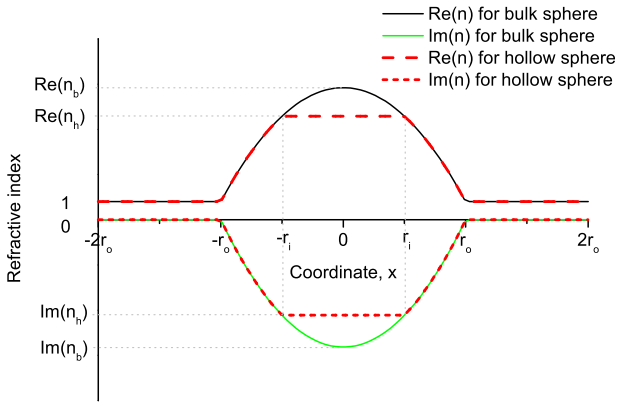

FIG. 3. Spatial dispersion of the homogenised refractive index described by Eq. (1). The values of maxima n_b and n_h were calculated from Eqs. (3) and (4).

spatial dispersion obeying Eq. (1). For calculating its R and T coefficients, the layer was first divided into N parts. Using Maxwell equations, it is possible to obtain the direct solutions for electric and magnetic fields at the boundaries of each thin layer. Written in matrix notations, they have the following form[11,15]

$$\begin{bmatrix} E_1 \\ H_1 \end{bmatrix} = \begin{bmatrix} \cos(k_t\tau_0) & i\sin(k_t\tau_0)k_0/k_t \\ i\sin(k_t\tau_0)k_t/k_0 & \cos(k_t\tau_0) \end{bmatrix} \begin{bmatrix} E_2 \\ H_2 \end{bmatrix}, \quad (5)$$

where E_1, H_1 and E_2, H_2 are electric and magnetic field in the left and right side of a layer of thickness τ_0, $k_t = \frac{2\pi}{\lambda a}\sqrt{n(x)^2a^2 - \lambda^2/4}$ and $k_0 = \frac{2\pi}{\lambda a}\sqrt{n_0^2a^2 - \lambda^2/4}$ are the wave vectors in the layer of refractive index $n(x)$ and in air (refractive index $n_0 = 1$) inside the waveguide of width $a = 7.2$ mm, respectively; λ being the wavelength. The first term in the right part of Eq. (5) is known as the characteristic matrix of the layer.

In the case of a multi-layered structure, the characteristic matrix of the whole layer is the product of all single layer matrices. The R, T coefficients of the N-layered subsystem inside the waveguide can be calculated as

$$R = S_{11}^2 = (n_0 - C/B)^2/(n_0 + C/B)^2, \quad (6)$$

$$T = S_{21}^2 = 4n_0^2/(n_0B + C)^2, \quad (7)$$

where

$$\begin{bmatrix} B \\ C \end{bmatrix} = \left\{ \prod_{t=1}^{N} \begin{bmatrix} \cos(k_t\tau) & i\sin(k_t\tau)k_0/k_t \\ i\sin(k_t\tau)k_t/k_0 & \cos(k_t\tau) \end{bmatrix} \right\} \begin{bmatrix} 1 \\ n_0 \end{bmatrix}. \quad (8)$$

In Fig. 4 are presented the measured and modelled Ka-band spectra of two different monolayers made from HS-A and HS-B with diameters D and shell thicknesses dr. A good agreement can be observed between the experiment and modelling for the reflection coefficient R. The possible reason for the difference between modelled and measured reflection coefficients in the high-frequency part in the spectra of Fig. 4 is the unevenness of shell thickness dr in the real spheres forming the monolayer. The experimental values of the transmission coefficient T are low, as expected, but considerably higher than those predicted by the model. This

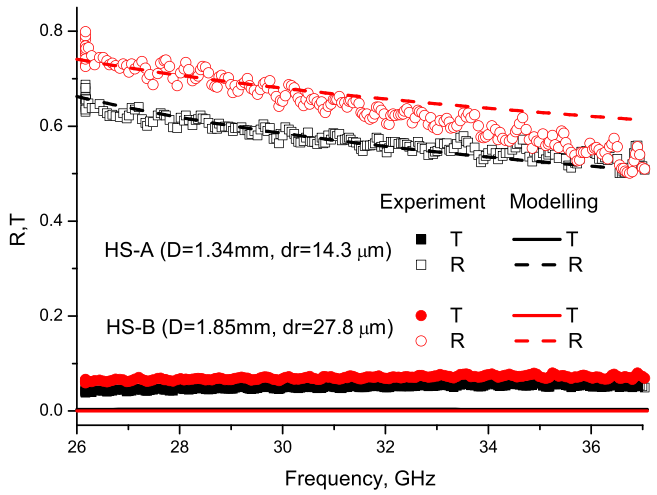

FIG. 4. Measured and modelled Ka-band spectra of hollow spheres with different diameter D and wall thicknesses dr.

might be due to a bad electrical contact between the HS monolayer and the walls of the waveguide.[1,5] The small gap between the waveguide and the sample leads to the penetration of electromagnetic radiation and therefore to an increase of transmission coefficient.

The model proposed above was applied to estimate how some changes in the carbon HS parameters (i.e., radius r_o and shell thickness dr) would affect the electromagnetic response of the corresponding monolayer. First, the HS radius was fixed, whereas the thickness of the shell dr was changed. The resultant spectra of R and T coefficients (not shown) are closely behaved as those presented in Fig. 4. R and T increased and decreased when dr increased, respectively. It is especially interesting to look at the absorption spectra $A = 1 - R - T$. For example, the calculated results for monolayers based on hollow spheres of constant radius $r_o = 0.67$ mm (corresponding to radius of HS-A) and variable shell thicknesses dr are presented in Fig. 5.

Fig. 5 shows that the absorption coefficient is the highest when the shell thickness dr ranges from 4 to 8 μm. From these results, it can be concluded that there is an optimal thickness leading to a maximal absorption of the monolayer formed by HS of radius $r_o = 0.67$ mm. When the shell

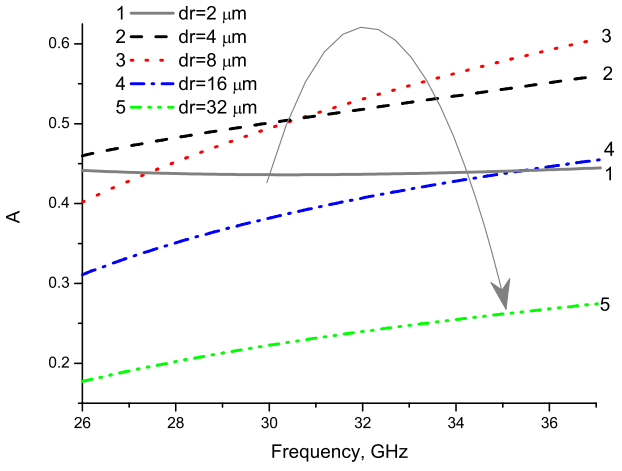

FIG. 5. Calculated absorption spectra of monolayers based on carbon hollow spheres of constant radius $r_o = 0.67$ mm and variable shell thicknesses dr.

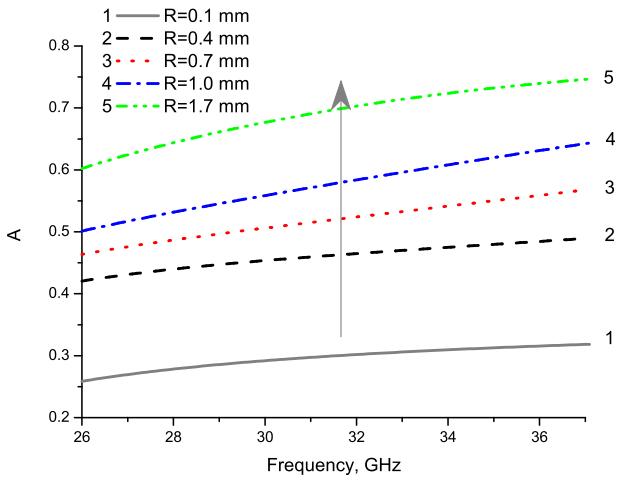

FIG. 6. Calculated absorption spectra of monolayers based on carbon hollow spheres of variable radii r_o and constant shell thickness $dr = 4\,\mu$m.

thickness was fixed at $dr = 4\,\mu$m while changing the radius of the hollow spheres in the monolayer, the results led to the absorption spectra shown in Fig. 6.

The analysis of Fig. 6 shows that an increase of sphere radius leads to a monotonic increase of absorption coefficient A. This is because the increase of sphere radius leads to an increase of the total thickness of the system and summary amount of carbon in the monolayer. It can be concluded from these data that, for EM absorption applications, spheres with larger diameters are to be preferred.

The frequency dependencies presented in Figs. 5 and 6 have generally the same appearance. For a clearer and more detailed analysis of these data, the frequency was fixed at 30 GHz, and both r_o and dr were varied, see Fig. 7.

Based on the results given in Fig. 7, it can be seen that the absorption coefficient presents a maximum for all varied values of r_o when dr is in range 5–10 μm. The maximum of absorption is especially explicit for smaller values of r_o. To explain the origin of this maximum, let us consider Eq. (4), where $r_o^2 - r_i^2 \approx 2r_o dr$, so that dr directly controls the real and imaginary parts of the refractive index of the carbon HS monolayer. A similar maximum was observed in thin film optics. It is indeed shown in Ref. 15 that, for each single homogeneous layer, there are existing relation between $Im(n)$ and $Re(n)$ for maximum absorption at fixed layer thickness. Generally, on one hand, the wall thickness dr controls the averaged conductivity and hence the energy losses in the monolayer of spheres. On the other hand, high values of averaged conductivity lead to increase of reflection and decrease of absorption coefficients.

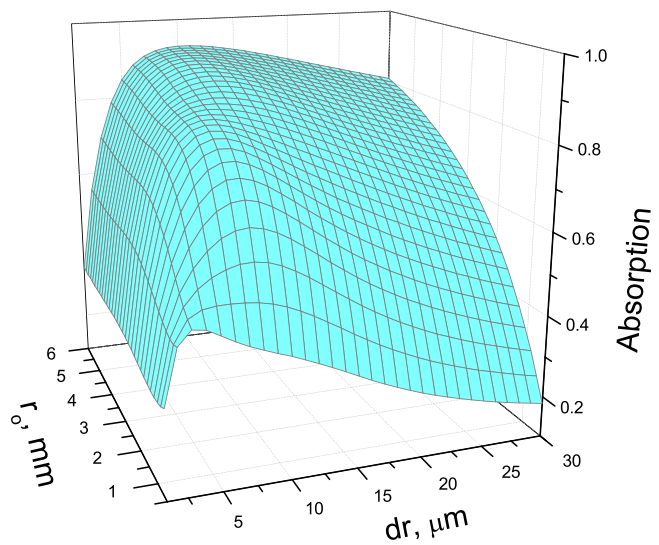

FIG. 7. Calculated absorption spectra of monolayers based on carbon hollow spheres at 30 GHz for various radii r_o and shell thicknesses dr.

Additionally, it can be seen from Fig. 7 that A increased with r_o. Therefore, for EM absorption applications, the most preferable hollow spheres are those having large radii r_o. Our model predicts that, for high values of r_o, it is possible to achieve almost perfect microwave absorption with $A > 95\%$. It is also worth mentioning, however, that high values of A are obtained when r_o starts to be comparable or larger than the wavelength of the initial radiation. In this case, the validity of the long-wave approximation used here should be experimentally proved by free-space measurements or more exact Mie scattering-based models[16] should be used.

The graphs corresponding to Fig. 7 calculated at 26 and 37 GHz have the same general form, but the maximum in the plane section $r_o = const$ is more explicit and narrow at 37 GHz, and broader and flattened at 26 GHz. Therefore, at higher frequencies, the electromagnetic response of the monolayer is more sensitive to changes of dr.

In summary, a model for describing the electromagnetic properties in Ka-band of monolayers based on a 2D packing of hollow carbon spheres was presented. The results showed that, for EM applications requiring high absorption, the most preferable hollow spheres are those of larger radii r_o. Additionally, it was estimated that, for each value of HS radius, there is an optimum shell thickness dr such that the absorption coefficient of the monolayer is the highest. The present work therefore pointed out that "moth-eye"-like 2D ordered structures based on hollow conducting spheres are promising systems for being used in microwave radiation absorption applications.

This work was supported in part by FP7-PEOPLE-2013-IRSES-610875 NAmiceMC, FP7 Twinning Grant Inconet EaP_004.

[1]D. Bychanok, A. Plyushch, K. Piasotski, A. Paddubskaya, S. Voronovich, P. Kuzhir, S. Baturkin, A. Klochkov, E. Korovin, M. Letellier, S. Schaefer, A. Szczurek, V. Fierro, and A. Celzard, Phys. Scr. **90**, 094019 (2015).
[2]A. Szczurek, A. Ortona, L. Ferrari, E. Rezaei, G. Medjahdi, V. Fierro, D. Bychanok, P. Kuzhir, and A. Celzard, Carbon **88**, 70 (2015).
[3]D. Bychanok, A. Plyushch, G. Gorokhov, V. Skadorov, P. Kuzhir, S. Maksimenko, J. Macutkevic, A. Ortona, L. Ferrari, E. Rezaei, A. Szczurek, V. Fierro, and C. A., in Proceedings of Electromagnetics in Advanced Applications and IEEE-APS Topical Conference on Antennas and Propagation in Wireless Communications, Italia, Torino, 7–11 September 2015.
[4]G. Tondi, V. Fierro, A. Pizzi, and A. Celzard, Carbon **47**, 1480 (2009).
[5]F. Moglie, D. Micheli, S. Laurenzi, M. Marchetti, and V. M. Primiani, Carbon **50**, 1972 (2012).
[6]D. Micheli, R. Morles, M. Marchetti, F. Moglie, and V. M. Primiani, Carbon **68**, 149 (2014).
[7]A. Mejdoubi and C. Brosseau, J. Appl. Phys. **100**, 094103 (2006).
[8]C.-H. Sun, P. Jiang, and B. Jiang, Appl. Phys. Lett. **92**, 061112 (2008).

[9]D. Stavenga, S. Foletti, G. Palasantzas, and K. Arikawa, Proc R. Soc. London, Ser. B **273**, 661 (2006).
[10]N. Klochko, G. Khrypunov, Y. Myagchenko, E. Melnychuk, V. Kopach, K. Klepikova, V. Lyubov, and A. Kopach, Semiconductors **48**, 531 (2014).
[11]M. Born and E. Wolf, *Principles of Optics*, 4th ed. (Pergamon Press, 1970).
[12]G. Bhatia, R. Aggarwal, M. Malik, and O. Bahl, J. Mater. Sci. **19**, 1022 (1984).
[13]D. F. Baker and R. H. Bragg, J. Non-Cryst. Solids **58**, 57 (1983).
[14]L. Pesin, J. Mater. Sci. **37**, 1 (2002).
[15]H. A. MacLeod, *Thin-Film Optical Filters*, 3rd ed. (CRC Press, 2001).
[16]G. Mie, Ann. Phys. **330**, 377 (1908).